






Cite this: *Chem. Sci.*, 2022, 13, 12527 All publication charges for this article have been paid for by the Royal Society of Chemistry

Dual role of benzophenone enables a fast and scalable C-4 selective alkylation of pyridines in flow†

Jesús Sanjosé-Orduna, ^{‡a} Rodrigo C. Silva, ^{‡ab} Fabian Raymenants, ^a Bente Reus,^a Jannik Thaens,^a Kleber T. de Oliveira ^b and Timothy Noël ^{*a}

The efficient C-4 selective modification of pyridines is a major challenge for the synthetic community. Current strategies are plagued with at least one drawback regarding functional group-tolerant electronic activation of the heteroarene, mild generation of the required alkyl radicals, regioselectivity, safety and/or scalability. Herein, we describe a fast, safe and scalable flow process which allows preparation of said C-4 alkylated pyridines. The process involves a photochemical hydrogen atom transfer (HAT) event to generate the carbon-centered radicals needed to alkylate the C-2 blocked pyridine. In a two-step streamlined flow process, this light-mediated alkylation step is combined with a nearly instantaneous inline removal of the blocking group. Notably, cheap benzophenone plays a dual role in the pyridine alkylation mechanism by activating the hydrocarbon feedstock reagents *via* a HAT mechanism, and by acting as a benign, terminal oxidant. The key role of benzophenone in the operative reaction mechanism has also been revealed through a combination of experimental and computational studies.

Received 7th September 2022

Accepted 8th October 2022

DOI: 10.1039/d2sc04990b

rsc.li/chemical-science

Introduction

Pyridines are privileged scaffolds and their incorporation into biologically-active molecules can dramatically improve their potency.¹ Hence, synthetic tools that can selectively edit this moiety are highly desired to enable the streamlined synthesis of various pharmaceuticals and agrochemicals.²

In the 1970s, Minisci and co-workers reported upon the thermal generation of alkyl radicals *via* decarboxylation of carboxylic acids using silver salts. These nucleophilic radicals were subsequently exploited to alkylate various heteroarenes, including pyridines, under strongly acidic and oxidative conditions.³ More than 50 years later, this strategy, coined as the Minisci reaction, still stands and has evolved into a key method for the modification of heteroarenes.⁴ However, between academic discovery and practical use in the pharmaceutical and agrochemical industry, there remain many roadblocks for the widespread implementation of the Minisci reaction. These challenges include (i) a functional-group tolerant electrophilic activation of the basic heteroarene, (ii)

a reliable and mild generation of the alkyl radicals; (iii) the poor regioselectivity of the radical addition to the aromatic ring⁵ leading to various byproducts and (iv) the safe and challenging scale up to relevant quantities for process chemists (Fig. 1A). In recent years, the use of bulky, C-2 blocking groups has proven to be very effective to enable both regioselectivity towards the C-4 position and efficient electrophilic activation of the pyridine moiety (Fig. 1B).⁶

With respect to the generation of radicals, since the initial thermal decarboxylation methodology developed by Minisci, several milder strategies have been discovered. As a prime example, photocatalysis has emerged in the past decade as a powerful tool for the efficient formation of open-shell reactive intermediates.⁷ Among the different radical precursors available, the direct activation of ubiquitous C–H bonds is perhaps one of the most desirable synthetic targets, as it bypasses the need for lengthy pre-functionalization steps. The homolytic cleavage of such inert C–H bonds *via* hydrogen atom transfer (HAT) has recently been shown to be a very powerful approach to enable both early and late stage functionalization of hydroalkanes.⁸

However, the coupling of the HAT-generated radical with activated pyridines is so far an underdeveloped strategy (Fig. 1C). Few examples are reported in the literature, usually requiring excess of hydrocarbons, inert conditions, transition metals and/or very extended reaction times, making such strategies less practical. Consequently, in order to make the transition from academic discovery to a scalable process, synthetic methodologies are urgently needed that use cheap

^aFlow Chemistry Group, Van't Hoff Institute for Molecular Sciences (HIMS), University of Amsterdam, Science Park 904, 1098 XH Amsterdam, The Netherlands. E-mail: t.noel@uva.nl; Web: <https://www.noelresearchgroup.com/>

^bDepartamento de Química, Universidade Federal de São Carlos, SP 13565-905, Brazil

† Electronic supplementary information (ESI) available: For the spectral data, experimental and computational experimental data. See DOI: <https://doi.org/10.1039/d2sc04990b>

‡ These authors contributed equally to this work.

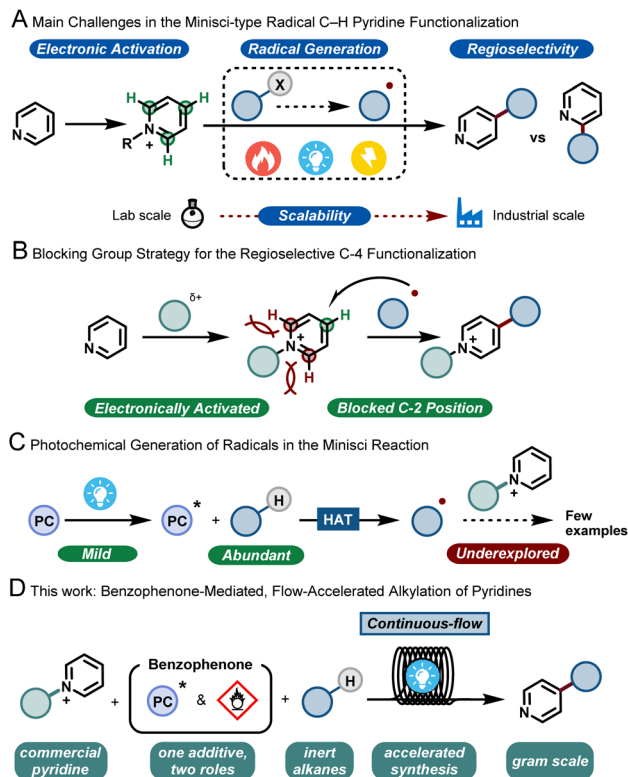


Fig. 1 C-4 selective alkylation of pyridines. (A) Main challenges in the Minisci-type pyridine functionalization reactions. (B) Blocking group strategy for the C-4 regioselective functionalization. (C) Photochemical generation of alkyl radicals in the Minisci reaction. (D) A benzophenone-mediated, flow-accelerated alkylation of blocked pyridines (this work).

and readily-available starting materials, involve few and non-toxic additives, require short reaction times and are scalable.

Given the experience of our group in developing multidisciplinary synthetic approaches,⁹ we wondered if the aforementioned issues could be simultaneously solved by developing a continuous-flow synthetic strategy. Flow technology has been shown to uniquely pair with photochemistry, by effectively reducing the reaction times, by improving reaction selectivity due to excellent mass and photon transfer characteristics, and by enabling facile scale up.¹⁰ Moreover, using such a flow strategy would also enable us to combine both the photochemical C-4 functionalization of the pyridine and the subsequent removal of the C-2 blocking group, ultimately delivering an operationally simple process that should ensure the preparation of large quantities of C-4 alkylated pyridines using hydrocarbons as cheap and abundantly available coupling partners (Fig. 1D).

Discussion

With this blueprint in mind, we commenced our investigations by testing a model system consisting of a commercially available C2-blocked pyridine **1**,^{6h} cyclohexane **2a**, tetrabutylammonium decatungstate (TBADT) as the HAT photocatalyst¹¹ and stoichiometric amounts of a terminal oxidant, *i.e.* (NH₄)₂S₂O₈.

Table 1 Optimization of reaction conditions for the C–C bond-forming step

Entry	2a (eq.)	HAT mediator	Oxidant	3a ^a [%]
1	10	TBADT (4 mol%)	(NH ₄) ₂ S ₂ O ₈ (2 eq.)	24 ^b
2	10	BP1 (20 mol%)	(NH ₄) ₂ S ₂ O ₈ (2 eq.)	28 ^b
3	20	BP1 (20 mol%)	Oxygen	0
4	10	BP1 (20 mol%)	None	13
5	10	BP1 (1 eq.)		63
6	10	BP2 (1 eq.)		36
7	10	BP3 (1 eq.)		52
8	10	BP4 (1 eq.)		55
9	2.5	BP1 (1.5 eq.)		70
10	2.5	BP1 (1.5 eq.)		27 ^c
11	2.5	None		0

^a Yields determined by ¹H NMR spectroscopy using 1,3,5-trimethoxybenzene as external standard. ^b Ammonium persulfate required a CH₃CN : H₂O (1 : 1) mixture as solvent for solubility issues. ^c In batch (See ESI† for further details).

BP1, R₁ = R₂ = H
BP2, R₁ = R₂ = MeO
BP3, R₁ = R₂ = CF₃
BP4, R₁ = MeO; R₂ = CF₃

^a Yields determined by ¹H NMR spectroscopy using 1,3,5-trimethoxybenzene as external standard. ^b Ammonium persulfate required a CH₃CN : H₂O (1 : 1) mixture as solvent for solubility issues. ^c In batch (See ESI† for further details).

We subjected the initial reaction mixture under air in a continuous-flow microreactor (ID = 0.8 mm, 3.3 mL) and exposed it to UV-A light irradiation (λ = 365 nm, 60 W input power) (See ESI† for details). Under these conditions, we could observe the regioselective C-4 alkylation of **1** albeit with a low yield for **3a** (Table 1, entry 1). In addition, precipitation of the photocatalyst and the oxidant in the reaction coil was observed, which would lead to clogging problems over time.¹² We wondered if the highly-charged nature of TBADT could be an issue under these conditions, so we decided to switch to a simpler organic HAT mediator, such as benzophenone (**BP1**).^{13,14} Although similar low yields were obtained (Table 1, entry 2), a completely homogeneous solution was observed during the entire experiment.

After selecting **BP1** as the HAT mediator, different oxidants and solvents were screened (see ESI† for details). Unexpectedly, when using oxygen as oxidant, the reaction was completely suppressed (Table 1, entry 3). Notably, a blank experiment revealed another interesting observation: without the addition of any external oxidant, we observed the formation of **3a** in 13% yield using 20 mol% of **BP1** (Table 1, entry 4). This finding, in combination with entry 3, prompted us to question if benzophenone could also act as a terminal oxidant. When repeating the reaction with a stoichiometric amount of **BP1**, the product **3a** was obtained in 63% yield, demonstrating the ability of **BP1** to not only engage in the C(sp³)–H activation event, but also to serve as terminal oxidant (Table 1, entry 5). Next, we evaluated a diverse set of substituted benzophenones. Electron-rich (**BP2**,

Table 1, entry 6), electron-poor (BP3, Table 1, entry 7) and a push–pull system (BP4, Table 1, entry 8) were subjected to the reaction conditions, but none of them outperformed the non-substituted and commercially available **BP1** as mediator. Finally, increasing the amount of **BP1** to 1.5 equivalents allowed us to decrease the equivalents of the hydroalkane **2a** to 2.5 equivalents, delivering the target compound **3a** in 70% yield (Table 1, entry 9).

This result was obtained without any special precautions during the reaction preparation, including the use of wet reagents/solvents and working under air, making our reaction protocol particularly user-friendly. Interestingly, when repeating the reaction under conventional batch conditions, the yield for the benzophenone-mediated alkyl–pyridyl coupling dropped to 27% (Table 1, entry 10), highlighting the importance of an efficient irradiation of the reaction mixture under microfluidic conditions. No reactivity was observed when the reaction was performed without **BP1** (Table 1, entry 11). Having found proper reaction conditions for the alkyl–pyridyl bond-forming reaction, we next aimed to remove the C2-blocking group attached to the pyridine moiety. To do so, we merged the reaction stream exiting the photochemical flow reactor with a dichloromethane solution containing the organic base 1,8-diazabicyclo[5.4.0]undec-7-ene (DBU). In only 20 min overall residence time, we could perform both the photomediated alkylation and the removal of the blocking group without the need for intermediate isolation. In addition, this operationally simple protocol also allowed us to scale up the process without re-optimization of the reaction conditions, which often plagues conventional batch scale up procedures. Simply by continuously pumping starting materials

into the reactor assembly, we could scale up the reaction to a gram-scale, with even slightly higher reaction yields (74% isolated yield for **4a**, 91% purity, 210 mg hour^{−1}).

The scope of pyridines that can be C-4 alkylated using our protocol is illustrated in Fig. 2. First, a diverse set of hydrocarbons bearing strong, non-activated C(sp³)–H bonds (**4a–4l**) were subjected to the photochemical reaction conditions. Benzophenone was able to cleave the C(sp³)–H bond in various cyclic alkane feedstocks, such as cyclopentane (**4b**), cycloheptane (**4c**), cyclooctane (**4d**), adamantane (**4g**), norbornane (**4h**), decalin (**4i**) and cyclododecane (**4j**) and the ensuing nucleophilic radical was subsequently coupled with the C2-blocked pyridine.

Also, linear alkanes, such as isopentane (**4k**) and *n*-pentane (**4l**), were selectively activated by benzophenone at their most hydridic C(sp³)–H bonds. Various amides, including dimethylformamide (DMF, **4m**) and dimethylacetamide (DMA, **4n**), could be activated α -to-N C(sp³)–H. Furthermore, 5 and 6-membered lactams (**4o–4r**), lactones (**4s**) and esters (**4t**) were compatible with our HAT-induced Minisci protocol. Notably, the sesquiterpene lactone natural product sclareolide (**4u**) could be regioselectively pyridinylated, demonstrating the potential of this protocol to act as a late-stage functionalization method. Finally, various C-3 substituted pyridines (**4v–4x**) were also compatible with the reaction conditions, giving rise to the corresponding C-4 alkylated compounds in good isolated yields. Unfortunately, alkanes bearing cyclic amines, cyclic ethers, aromatic rings or halogens gave rise to either low yields or complex reaction mixtures (see ESI† for details).

Next, we sought to investigate the mechanism of this process and, in particular, to elucidate the role of benzophenone. Using

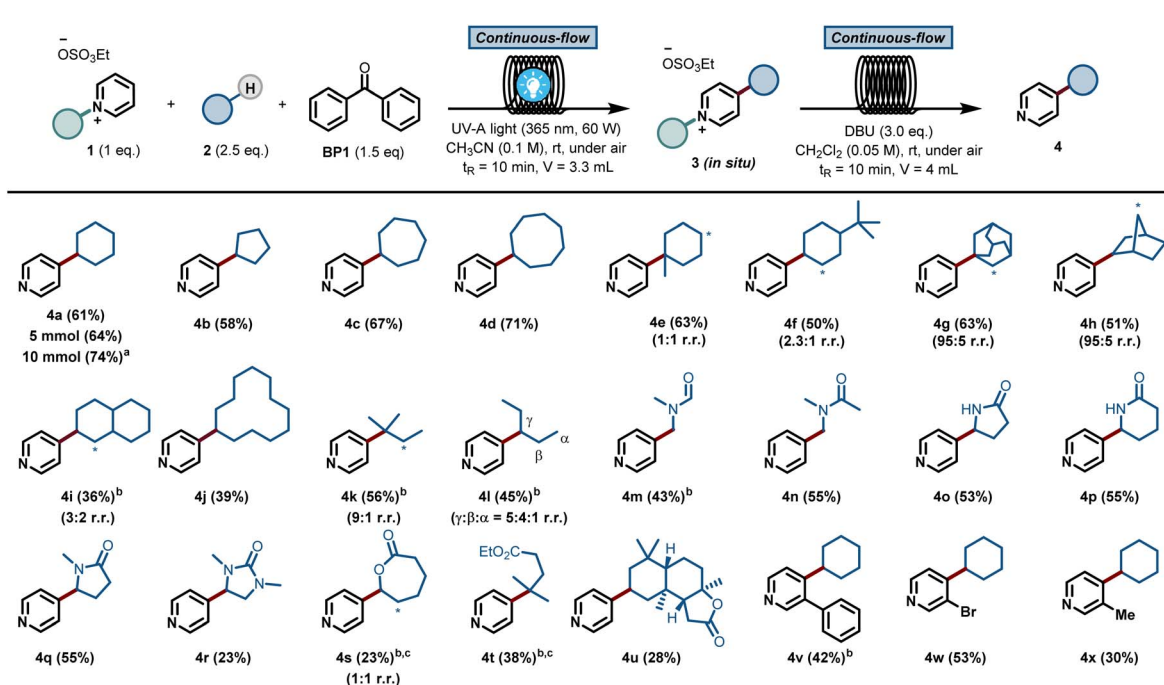


Fig. 2 Substrate scope of the benzophenone-mediated alkylation of pyridines with subsequent deprotection step. Reaction conditions: 0.5 mmol of **1**, 1.25 mmol of **2**, 0.75 mmol of **BP1** in CH₃CN (3 mL) and using 1.5 mmol of DBU in 5 mL of CH₂Cl₂ for the deprotection step. Isolated yield in brackets. * Indicates the position of the minor regioisomer formed; (a) 10 mmol scale, (b) 10 equiv. of **2**; (c) 1 h of residence time in the first step.

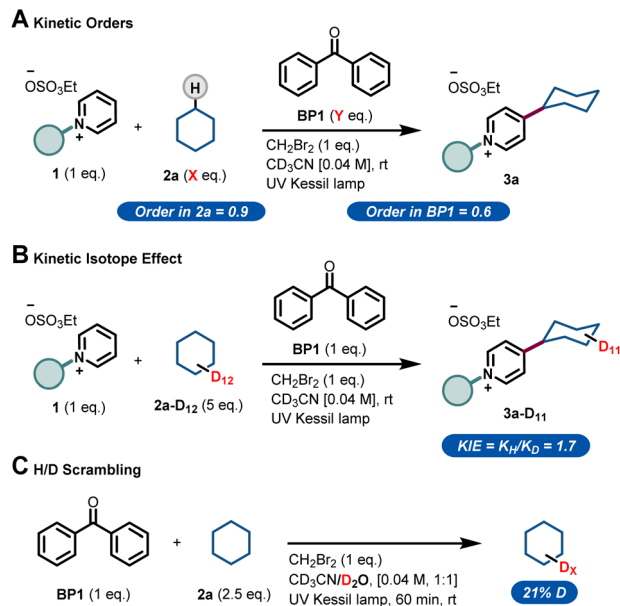


Fig. 3 Experimental mechanistic investigations. (A) Kinetic orders. (B) Kinetic Isotope Effect (KIE). (C) H/D scrambling.

the initial rates method we could extract the experimental reaction rates at different concentrations (Fig. 3A).¹⁵ From these kinetic investigations, the reaction order of cyclohexane was determined to be 0.9, suggesting a first-order dependence regarding the hydrocarbon concentration under these conditions.

Interestingly, the kinetic order of **BP1** was measured to be 0.6. This fractional order suggests that the role of benzophenone is more complex, and implies that **BP1** might be involved in different elementary steps through the entire mechanistic scenario. Similarly, to get further insights about the initial C(sp³)-H bond cleavage of cyclohexane, we examined the kinetic isotope effect (KIE) (Fig. 3B). To do that, we compared the initial rates of both a standard reaction and a reaction using deuterated cyclohexane (**2a-d₁₂**). A KIE of 1.7 was determined, which suggests that the C(sp³)-H bond cleavage of the alkane might be involved in the rate-determining step.¹⁶ Further H/D scrambling experiments demonstrated the reversibility of the process under the described reaction conditions, as we observed partial deuteration of cyclohexane when repeating the reaction using D₂O as cosolvent (Fig. 3C).

To further understand the experimentally-obtained mechanistic insights, we decided to simulate a plausible scenario that could explain this dual role of the benzophenone using density functional theory (DFT) calculations. The obtained qualitative reaction profile with the corresponding energies is depicted in Fig. 4 (See ESI† for further computational details). The reaction kicks off with UVA-light photoexcitation of the ground state benzophenone **BP1** to its triplet state **BP1***. This highly electrophilic species, regarded as the 0.0 in the energy profile, is responsible for the homolytic cleavage of a C(sp³)-H bond in the alkyl partner **Cy1**, through **TS1** at 11.3 kcal mol⁻¹. This low energetic barrier is in agreement with the absence of a primary KIE (Fig. 3B). The ensuing carbon-centered radical **Cy2** resides

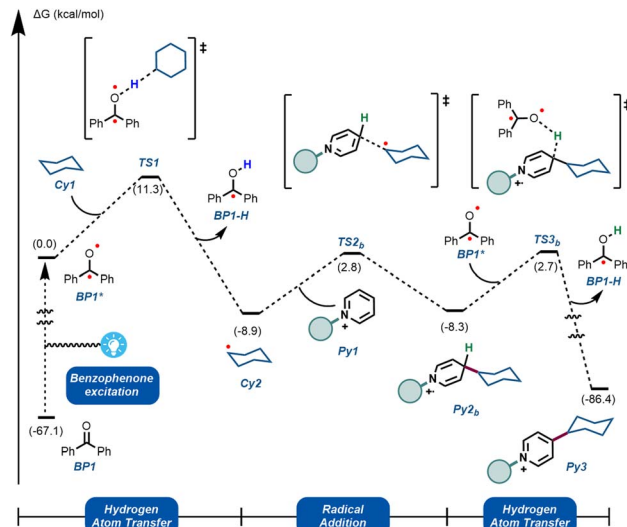


Fig. 4 Computational mechanistic investigations. Calculations were performed at the ωB97X-D/6-31+G(d,p)/CPCM (acetonitrile) level of theory. See ESI† for computational details.

in an endergonic position (−8.9 kcal mol⁻¹) relative to **BP1***. The reversibility of this step was observed experimentally (Fig. 3C), demonstrating that the reverse energetic barrier (20.2 kcal mol⁻¹) can be overcome at room temperature under the described reaction conditions.

Subsequently, species **Cy2** can engage in a radical addition at the only electronically and sterically accessible position of **Py1**, through **TS2b**. Given that the reversibility of **TS1** was demonstrated experimentally under these conditions, we can assume that the energetic barrier for **TS2b** (11.7 kcal mol⁻¹) is also within reach. Finally, we simulated the re-aromatization of the reduced **Py2b** by a second molecule of **BP1*** via a second hydrogen atom transfer event in **TS3b**. The energetic barrier for this last step from **Cy2** (11.0 kcal mol⁻¹) is comparable to **TS2b** and to **TS1**, showcasing that all the elementary steps are feasible at room temperature. This demonstrates that **BP1*** can participate not only in the first HAT reaction, but also in the terminal oxidation of **Py2b**, thus explaining the fractional kinetic order observed experimentally (Fig. 3A).

Combining all experimental and computational evidence, we can portray a plausible reaction mechanism for the benzophenone-enabled photomediated C4-alkylation of pyridines (Fig. 5). A photoexcited ketone in the triplet state **BP1*** is responsible for the cleavage of the strong C(sp³)-H bond via HAT, giving rise to a nucleophilic alkyl radical and concomitant formation of **BP1-H**. It should be noted that this protonated species can be re-oxidized to the original benzophenone under an oxygen atmosphere, leading to a catalytic pathway.^{14f} However, this reoxidation pathway is particularly slow as shown by our experiments, making it less practical for scale up (see ESI†). The generated alkyl radical is subsequently added to the activated pyridine, establishing the targeted alkyl-pyridyl bond. Finally, the ensuing radical cation has to be rearomatized. Notably, this is the specific step that often requires harsh, external oxidants in many Minisci reaction protocols. However,



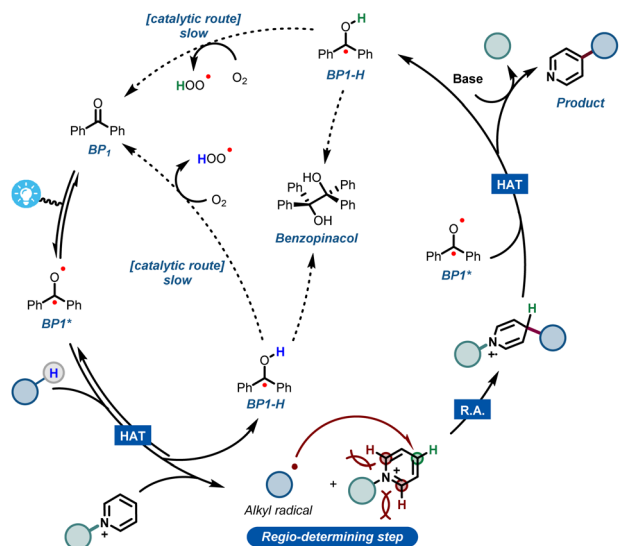


Fig. 5 Plausible mechanistic hypothesis for the benzophenone-mediated photoalkylation of pyridines.

under our set of reaction conditions, this step can be carried out mildly using a second molecule of **BP1***.

It is worth noting that oxygen is also capable of engaging into this oxidation step, but again requiring quite long reaction times. The second molecule of reduced **BP1-H** can be re-oxidized in the same fashion by oxygen, closing what happens to be a rather slow, catalytic cycle.

Additionally, during our optimizations with **BP1**, we observed the formation of small quantities of the dimerized benzopinacol derivative. This evidence also corroborates with the proposed radical **BP1-H** and with the need for more than 1 eq. of **BP1**, thus suggesting a competition between the re-oxidation of **BP1-H** by O_2 and its radical recombination (Fig. 5). Finally, the removal of the blocking group using a non-nucleophilic organic base gives rise to the desired C-4 alkylated pyridine.

Conclusions

In conclusion, we have developed an efficient, safe and scalable two-step flow protocol to enable the C-4 selective alkylation of pyridines. The uninterrupted process involves a benzophenone-induced HAT generation of radicals, a subsequent alkylation of a C-2 blocked pyridine and the ultimate removal of the blocking group, requiring only 20 min of reaction time in total. The scope of this transformation is broad, and the targeted pyridines can be alkylated with a variety of activated and non-activated hydrocarbon feedstocks. Finally, a combined experimental and computational mechanistic investigation was carried out to elucidate the reaction mechanism and to highlight the role of benzophenone as HAT reagent and mild oxidant.

Data availability

Experimental details, used materials, sample preparation and analytical data (NMR) for the compounds **4a–4x**. All the raw

computational data is available on the ioChem-BD¹⁷ repository and can be freely accessed at <https://doi.org/10.19061/iochem-bd-6-156>.

Author contributions

J. S.-O. conceived the idea for this work. J. S.-O. and J. T. carried out initial optimization studies. R. C. S. developed the refined reaction conditions and the substrate scope, with the help of B. R. and J. S.-O. carried out the experimental and computational mechanistic studies. F. R. and B. R. studied the effect of oxygen in the reaction. T. N. provided direction for the scientific strategy. J. S.-O. and T.N. wrote the manuscript with input from all the authors.

Conflicts of interest

There are no conflicts to declare.

Acknowledgements

R. C. S. scholarship was provided by the São Paulo Research Foundation – FAPESP – (grant numbers: 2021/09145-8), and thanks are also due to the Coordenação de Aperfeiçoamento de Pessoal de Nível Superior – Brasil (CAPES) – Financial Code 001. The authors would also like to acknowledge kind financial support from the European Union (FLIX, No. 862179, F. R. and T. N.).

Notes and references

- (a) E. Vitaku, D. T. Smith and J. T. Njardarson, *J. Med. Chem.*, 2014, **57**, 10257–10274; (b) Y. Ling, Z. Y. Hao, D. Liang, C. L. Zhang, Y. F. Liu and Y. Wang, *Drug Des. Devel. Ther.*, 2021, **15**, 4289–4338; (c) P. Bhutani, G. Joshi, N. Raja, N. Bachhav, P. K. Rajanna, H. Bhutani, A. T. Paul and R. Kumar, *J. Med. Chem.*, 2021, **64**, 2339–2381.
- (a) T. Cernak, K. D. Dykstra, S. Tyagarajan, P. Vachal and S. W. Krska, *Chem. Soc. Rev.*, 2016, **45**, 546–576; (b) J. Boström, D. G. Brown, R. J. Young and G. M. Keserü, *Nat. Rev. Drug Discovery*, 2018, **17**, 709–727; (c) L. Zhang and T. Ritter, *J. Am. Chem. Soc.*, 2022, **144**, 2399–2414.
- (a) F. Minisci, R. Galli, M. Cecere, V. Malatesta and T. Caronna, *Tetrahedron Lett.*, 1968, **54**, 5609–5612; (b) F. Minisci, R. Galli, V. Malatesta and T. Caronna, *Tetrahedron*, 1970, **26**, 4083–4091; (c) F. Minisci, R. Bernardi, F. Bertini, R. Galli and M. Perchinummo, *Tetrahedron*, 1971, **27**, 3575–3579.
- For selected reviews about the Minisci reaction: (a) M. A. J. Dunston, *Med. Chem. Comm.*, 2011, **2**, 1135–1161; (b) A. C. Sun, R. C. McAtee, E. J. McClain and C. R. J. Stephenson, *Synthesis*, 2019, **51**, 1063–1072; (c) R. S. J. Proctor and R. J. Phipps, *Angew. Chem., Int. Ed.*, 2019, **58**, 13666–13699.
- (a) F. O'Hara, D. G. Blackmond and P. S. Baran, *J. Am. Chem. Soc.*, 2013, **135**, 12122–12134; (b) A. de A. Bartolomeu,



- R. C. Silva, T. J. Brocksom, T. Noël and K. T. de Oliveira, *J. Org. Chem.*, 2019, **84**, 10459–10471.
- 6 (a) Y. Nakao, Y. Yamada, N. Kashihara and T. Hiyama, *J. Am. Chem. Soc.*, 2010, **132**, 13666–13668; (b) P. S. Fier, *J. Am. Chem. Soc.*, 2017, **139**, 9499–9502; (c) Y. Moon, B. Park, I. Kim, G. Kang, S. Shin, D. Kang, M. H. Baik and S. Hong, *Nat. Comm.*, 2019, **10**, 4117; (d) I. Kim, S. Park and S. Hong, *Org. Lett.*, 2020, **22**, 8730–8734; (e) W. Lee, S. Jung, M. Kim and S. Hong, *J. Am. Chem. Soc.*, 2021, **143**, 3003–3012; (f) S. Shin, S. Lee, W. Choi, N. Kim and S. Hong, *Angew. Chem., Int. Ed.*, 2021, **60**, 7873–7879; (g) B. Kweon, C. Kim, S. Kim and S. Hong, *Angew. Chem., Int. Ed.*, 2021, **60**, 26813–26821; (h) J. Choi, G. Laudadio, E. Godineau and P. S. Baran, *J. Am. Chem. Soc.*, 2021, **143**, 11927–11933; (i) H. Choi, G. R. Mathi, S. Hong and S. Hong, *Nat. Comm.*, 2022, **13**, 1776; (j) Z. Zhang, Q. He, X. Zhang and C. Yang, *Org. Biomol. Chem.*, 2022, **20**, 1969–1973.
- 7 (a) T. P. Yoon, M. A. Ischay and J. Du, *Nat. Chem.*, 2010, **2**, 527–532; (b) D. Staveness, I. Bosque and C. R. J. Stephenson, *Acc. Chem. Res.*, 2016, **49**, 2295–2306; (c) W.-M. Cheng, R. Shang, M.-C. Fu and Y. Fu, *Chem. Eur. J.*, 2017, **23**(11), 2537–2541; (d) W.-M. Cheng, R. Shang and Y. Fu, *ACS Catal.*, 2017, **7**, 907–911; (e) S. Crespi and M. Fagnoni, *Chem. Rev.*, 2020, **120**, 9790–9833; (f) R. Cannalire, S. Pelliccia, L. Sancineto, E. Novellino, G. C. Tron and M. Giustiniano, *Chem. Soc. Rev.*, 2021, **50**, 866–897; (g) L. Candish, K. D. Collins, G. C. Cook, J. J. Douglas, A. Gómez-Suárez, A. Jolit and S. Keess, *Chem. Rev.*, 2022, **122**, 2907–2980.
- 8 For reviews about the use of hydrogen atom transfer for the generation of radicals see: (a) H. Cao, X. Tang, H. Tang, Y. Yuan and J. Wu, *ChemCatChem*, 2021, **1**, 523–598; (b) L. Capaldo, D. Ravelli and M. Fagnoni, *Chem. Rev.*, 2022, **122**, 1875–1924.
- 9 (a) G. Laudadio, S. Govaerts, Y. Wang, D. Ravelli, H. F. Koolman, M. Fagnoni, S. W. Djuric and T. Noël, *Angew. Chem., Int. Ed.*, 2018, **57**, 4078–4082; (b) G. Laudadio, Y. Deng, K. van der Wal, D. Ravelli, M. Nuño, M. Fagnoni, D. Guthrie, Y. Sun and T. Noël, *Science*, 2020, **369**, 92–95; (c) T. Wan, L. Capaldo, G. Laudadio, A. V. Nyuchev, J. A. Rincón, P. García-Losada, C. Mateos, M. O. Frederick, M. Nuño and T. Noël, *Angew. Chem., Int. Ed.*, 2021, **60**, 17893–17897; (d) D. Mazzarella, A. Pulcinella, L. Bovy, R. Broersma and T. Noël, *Angew. Chem., Int. Ed.*, 2021, **60**, 21277–21282; (e) L. Capaldo, S. Bonciolini, A. Pulcinella, M. Nuño and T. Noël, *Chem. Sci.*, 2022, **13**, 7325–7331.
- 10 (a) B. Gutmann, D. Cantillo and C. O. Kappe, *Angew. Chem., Int. Ed.*, 2015, **54**, 6688–6728; (b) M. B. Plutschack, B. Pieber, K. Gilmore and P. H. Seeberger, *Chem. Rev.*, 2017, **117**, 11796–11893; (c) S. Govaerts, A. Nyuchev and T. Noël, *J. Flow. Chem.*, 2020, **10**, 13–71; (d) Z. Dong, Z. Wen, F. Zhao, S. Kuhn and T. Noël, *Chem. Eng. Sci. X*, 2021, **10**, 100097; (e) L. Buglioni, F. Raymenants, A. Slattery, S. D. A. Zondag and T. Noël, *Chem. Rev.*, 2022, **122**, 2752–2906.
- 11 (a) M. C. Quattrini, S. Fujii, K. Yamada, T. Fukuyama, D. Ravelli, M. Fagnoni and I. Ryu, *Chem. Commun.*, 2017, **53**, 2335–2338; (b) D. Ravelli, M. Fagnoni, T. Fukuyama, T. Nishikawa and I. Ryu, *ACS Catal.*, 2018, **8**, 701–713.
- 12 (a) Z. Dong, S. D. A. Zondag, M. Schmid, Z. Wen and T. Noël, *Chem. Eng. J.*, 2022, **428**, 130968; (b) A. Chaudhuri, S. D. A. Zondag, J. H. A. Schuurmans, J. van der Schaaf and T. Noël, *Org. Proc. Res. Dev.*, 2022, **26**, 1279–1288.
- 13 (a) J. Pérez-Prieto, R. E. Galian and M. A. Miranda, *Mini Rev. Org. Chem.*, 2006, **3**, 117–135; (b) G. Dormán, H. Nakamura, A. Pulsipher and G. D. Prestwich, *Chem. Rev.*, 2016, **116**, 15284–15398; (c) J. Mateos, S. Cuadros, A. Vega-Peñaloza and L. Dell'amico, *Synlett*, 2022, **33**, 116–128.
- 14 For some selected examples of aromatic ketones acting as a hydrogen atom transfer mediator see: (a) C. B. Tripathi, T. Ohtani, M. T. Corbett and T. Ooi, *Chem. Sci.*, 2017, **8**, 5622–5627; (b) Y. Shen, Y. Gu and R. Martin, *J. Am. Chem. Soc.*, 2018, **140**, 12200–12209; (c) Y. Li, M. Lei and L. Gong, *Nat. Catal.*, 2019, **2**, 1016–1026; (d) C. Y. Huang, J. Li, W. Liu and C. J. Li, *Chem. Sci.*, 2019, **10**, 5018–5024; (e) Y. Gu, H. Yin, M. Wakeling, J. An and R. Martin, *ACS Catal.*, 2022, **12**, 1031–1036; (f) A. Luridiana, D. Mazzarella, L. Capaldo, J. A. Rincon, P. Garcia-Losada, C. Mateos, M. O. Frederick, M. Nuno, W. J. Buma and T. Noël, *ACS Catal.*, 2022, **12**, 11216–11225; (g) L. Zhang, B. Pfund, O. S. Wenger and X. Hu, *Angew. Chem., Int. Ed.*, 2022, **61**, e202202649.
- 15 When measuring the kinetic orders of a photochemical reaction, the absorption of a photon by a molecule can be regarded as the first, bimolecular elementary reaction. Therefore, under controlled, identical light irradiation conditions, experimental apparent reaction rates can be compared. For further discussion see: (a) M. Hippler, *J. Chem. Educ.*, 2003, **80**, 1074–1077; (b) S. Toby, *J. Chem. Educ.*, 2005, **82**, 37–38.
- 16 E. M. Simmons and J. F. Hartwig, *Angew. Chem., Int. Ed.*, 2012, **51**, 3066–3072.
- 17 M. Álvarez-Moreno, C. de Graaf, N. López, F. Maseras, J. M. Poblet and C. Bo, *J. Chem. Inf. Model.*, 2015, **55**, 95–1035.

